Propagation of modulated waves in narrow-bandpass one-dimensional lattices

Serge Bruno Yamgoué,[1,*] Bonaventure Nana,[1,†] Guy Roger Deffo,[2,‡] and François Beceau Pelap[2,§]
[1]*Department of Physics, Higher Teachers Training College Bambili, University of Bamenda, P.O. Box 39, Bamenda, Cameroon*
[2]*Unité de Recherche de Mécanique et de Modélisation des Systèmes Physiques, Université de Dschang, BP 69 Dschang, Cameroun*

(Received 30 August 2019; published 24 December 2019)

We consider the problem of the propagation of modulated waves in one-dimensional discrete lattices with linear bandpass-type dispersion relation. We are interested specifically in the cases where the gap frequency f_0 and the cutoff frequency $f_{\max}$ verify $0 < f_0 < f_{\max} < 2f_0$. Analytical investigations of such models commonly use the rotating wave approximation in which only the fundamental harmonic is taken into consideration. This approach is routinely justified by the physical argument that the zeroth and higher harmonic frequency terms cannot propagate, being out of band. Using a simple model of electrical lattice as a case study, we show analytically that accounting for the generation of those terms is indispensable for the accurate prediction of modulated solitary waves supported by the model. Moreover, a carefully designed numerical investigation of the propagation of an exact and consistent second-order approximation of such waves reveals that the second-order harmonic included is transmitted throughout the network the same as the fundamental harmonic is. Thus, we unveil the pitfall of the rotating wave approximation that is detrimental to its reliability for most of the models to which it has commonly been employed. We also suggest how to avoid this pitfall.

DOI: 10.1103/PhysRevE.100.062209

I. INTRODUCTION

The probably first numerical experiment was performed as a means of studying the thermalization of energy in solids. A simple model consisting of a set of equal masses coupled to nearest neighbors by weakly nonlinear springs was used to check the conjecture that the energy imparted initially to a single normal mode of the system will uniformly spread throughout all its normal modes. Contrary to the expected equipartition of energy, it was rather observed that, in a periodic fashion, the energy spreads only to a few neighboring modes and returns almost entirely to the originally excited one. This phenomenon, nowadays called Fermi-Pasta-Ulam (FPU) recurrence, has largely contributed to the renewal of the attention devoted to the study of systems composed of a large number of interacting subsystems which are ordered in space. Since ever, nonlinear lattices have been at the heart of many extensive studies and are now established as the subject of a considerable multidisciplinary interest. This substantial interest stems, however, not only from a purely theoretical scientific curiosity such as understanding the FPU recurrence, but also from the viewpoint of their many interesting fields of application. In effect, one-dimensional monoatomic lattices of nonlinear oscillators have been used to model the energy transport in polypeptide chains in muscle proteins [1–3] or the energy transport in DNA [4]. Chains of coupled nonlinear electrical oscillators have been employed as equivalent electrical circuits for the investigation of transmission lines or long Josephson junctions [5]. Other examples include myelinated nerve fibers in biophysics [6], photonic crystals [7] and waveguides in optical devices [8], and arrays of microelectromechanical systems [9,10]. In this respect, arrays of nonlinear coupled particles continue to warrant and receive further attention.

As in the pioneering work of FPU, it is usually indispensable to resort to numerical experiments to investigate the numerous models that can be devised to describe actual physical problems of concern. Nevertheless, the importance of analytical investigation cannot be minimized. In fact, it is through the soliton theory which emerged from the analytical works of Zabusky and Kruskal that the FPU recurrence could be explained. This means that analytical analyses are useful for the appropriate interpretation of the results of numerical simulations. They can additionally constitute a guide for the latter as well as for experimental investigations. Yet, this necessary analytical investigation appears to be very challenging in general, due precisely to the two intrinsic features of these models, namely, the nonlinearity and the discreteness. In effect, apart from very few exceptions such as the Toda lattice [5], exactly integrable models which are also physically relevant are extremely scarce in the scientific literature.

Then to tackle analytically the investigation of the dynamics of lattices, several approximate techniques have been devised in order to manage to varied extents the intractability of their equations of motion. One of them, which seems to be among the best, is the so-called rotating wave approximation (RWA). In effect, neither the small amplitude assumption usually required by, e.g., the semidiscrete approximation nor the long-wavelength assumption required by the continuous medium approximation is a prerequisite for the application of the RWA. Moreover its usage encompasses the continuous envelope modulation in which it is combined with the

*sergebruno@yahoo.fr
†na1bo@yahoo.fr
‡guyrdeffo@yahoo.fr
§fbpelap@yahoo.fr; francois.pelap@univ-dschang.org

 ©2019 American Physical Society

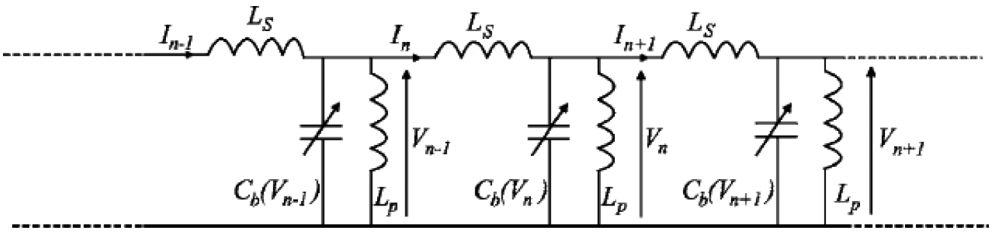

FIG. 1. Schematic of the discrete electrical transmission line.

Gardner-Morikawa transformation [11], as well as the fully discrete envelope modulation. We observe on the one hand that due to the nonlinearities of the system, higher-order harmonics are generated for each harmonic component of any finite amplitude wave that would be propagating in that system. On the other hand, RWA-based analyses consider only the fundamental harmonic component of the Fourier expansion of the wave function. Such analyses are usually performed for bandpass systems for which the gap frequency f_0 and the cutoff frequency $f_{\max}$ verify $0 < f_0 < f_{\max} < 2f_0$. Then, the argument that the bias term and the generated higher-order harmonic components cannot propagate because they are out of band is invoked to justify the validity of the use of the RWA for these narrow bandpass systems. To the best of our knowledge, however, no careful verification of it has ever been presented in these studies. One can then wonder whether this intuitive argument is absolutely free of pitfalls.

In this paper, we aim to address the suitability of the RWA for some of the models for which it has been employed in the current literature [12–16]. To this end, we consider here a simple model of a nonlinear electrical transmission line which satisfies the above narrowness condition. Then, by using the semidiscrete approximation we establish that it supports the propagation of solitonlike waves that can hardly be predicted using the RWA.

The organization of this paper is as follows. The specific discrete system considered for our investigation and the corresponding differential difference equations are presented in Sec. II. This is followed by the derivation, through a higher-order analysis, of a system of partial differential equations (PDEs) which govern the evolution of envelope waves in this lattice. A brief review of the modulational instability (MI) in the network based on these PDEs and the determination of their exact analytical solutions constitute the subject of Sec. III. These solutions are subsequently used to carry out direct numerical investigations whose outcomes are reported in Sec. IV. A brief discussion then follows in Sec. V to clarify the forms of model equations for which the shortcoming of the RWA shows up. In Sec. VI our conclusions are drawn.

II. MODEL AND EQUATION

Our model is the simple nonlinear discrete electrical transmission line schematically depicted in Fig. 1. Its unit cell comprises a series branch containing an inductor L_s, and a parallel branch containing another inductor L_p as well as a capacitor. Both inductors are assumed to be linear (their inductances are independent of voltage and current across them). But the capacitor which consists of the BB112 reversed-biased diode is, on the contrary, a nonlinear element. For the sake of clarity, we assume for the moment, following [5, Eq. (3.10)], that its capacitance-voltage relationship is approximated for low voltages V_n around the dc bias voltage V_b by

$$C_b(V_n) = C_0(1 - 2\alpha V_n), \tag{1}$$

where C_0 and α are constants and V_n is the voltage in the nth cell. In this paper, the numerical values assumed by the various electrical components mentioned above are as follows [14]: $L_s = 0.470$ mH, $L_p = 0.220$ mH, $C_0 = 320$ pF, and $\alpha = 0.21$ V^{-1}; the values of C_0 and α being determined for $V_b = 2$ V.

By applying Kirchhoff's laws, one can easily establish that the time dependence of the voltage V_n is governed by the following system of differential difference equations:

$$\frac{d^2}{dt^2}\left(V_n - \alpha V_n^2\right) + u_0^2(2V_n - V_{n+1} - V_{n-1}) + \omega_0^2 V_n = 0, \quad 1 \leqslant n \leqslant N \tag{2}$$

with $\omega_0 = (L_pC_0)^{-1/2}$, $u_0 = (L_sC_0)^{-1/2}$, and N the total number of cells in the lattice. In order to investigate the modulation of a wave carrier with angular frequency ω and wave number k in such lattices, it is customary [15,17–19] to introduce a fast scale variable $\theta = kn - \omega t$ and two additional, slow scale variables $\xi = \varepsilon(n - \mu t)$ and $\tau = \varepsilon^2 t$. Here ε is a dimensionless quantity which is assumed small in the sense that $0 < \varepsilon \ll 1$. The parameter μ is the linear group velocity, defined as the first derivative of a function $\omega = \omega(k)$ called linear dispersion relation. The latter is obtained by seeking plane-wave solutions to the lattice equation while assuming their amplitudes sufficiently small for the nonlinear terms to be neglected. In the case of Eq. (2), the linear dispersion relation and the corresponding group velocity are given, respectively, by

$$\omega^2 = \omega_0^2 + 4u_0^2 \sin^2\left(\frac{k}{2}\right), \quad \mu = \frac{u_0^2 \sin(k)}{\omega}. \tag{3}$$

This dispersion relation shows that admissible values for the frequency $f = \omega/2\pi$ of small amplitude plane waves that can propagate in the electrical lattice under consideration are in the range $f_0 = \omega_0/2\pi \leqslant f \leqslant f_{\max} = (\omega_0^2 + 4u_0^2)^{1/2}/2\pi$. Thus, as illustrated in Fig. 2, our system is a bandpass filter with a gap f_0 which is the lower cutoff angular frequency introduced by the parallel inductance L_p and an upper cutoff angular frequency $f_{\max}$ which is due to the discreteness effects. For the values of the line's parameters considered in this work, one has $f_0 = 0.600$ MHz and $f_{\max} = 1.017$ MHz, and correspondingly, $\omega_0 = 3.77 \times 10^6$ rad/s and

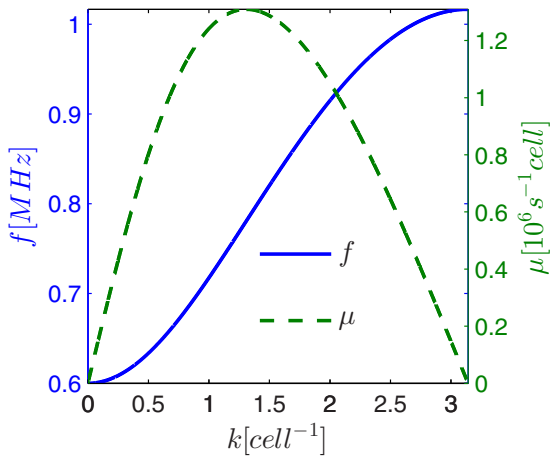

FIG. 2. Variations of the frequency (solid line) and group velocity (dashed line) as functions of wave number.

$\omega_{\max} = 6.39 \times 10^6$ rad/s. So the bandwidth is narrow since $f_{\max} = 1.69 f_0 < 2 f_0$.

In this paper we seek approximate solutions to Eq. (2) whose expressions in terms of the above fast and slow scale variables are of the form

$$V(\theta, \xi, \tau) = \varepsilon(Ae^{i\theta} + G_{10}) + \varepsilon^2(G_{20} + Be^{i\theta} + E_{22}e^{2i\theta}) + \varepsilon^3\left(G_{30} + Ce^{i\theta} + E_{32}e^{2i\theta} + E_{33}e^{3i\theta}\right) + \text{c.c.}, \tag{4}$$

where i is the imaginary unit (i.e., $i^2 = -1$) and all of A, B, C, G_{10}, G_{20}, E_{22}, G_{30}, E_{32}, and E_{33} are complex-valued functions of ξ and τ to be determined. As usual, c.c. is shorthand for *complex conjugate of the preceding terms*.

We remark that the fundamental harmonic $e^{i\theta}$ is rarely considered at higher order in the assumed forms of solution (or *Ansätze*). That is, the B and C terms are usually omitted in most of works found in the literature. Notable exceptions are those where weak amplitude solutions that oscillate around a steady state $V^{(0)}$ (which is zero in our case) are initially assumed in the form

$$V(\theta, \xi, \tau) = V^{(0)} + \sum_{m=1}^{\infty} \varepsilon^m \sum_{l=-m}^{m} V_l^{(m)}(\xi, \tau) e^{li\theta}, \tag{5}$$

where $V_l^{(m)}$ is a complex function and $V_l^{(m)}(\xi, \tau) = \overline{V_{-l}^{(m)}}(\xi, \tau)$ with the overbar denoting complex conjugation. They include the papers by Ichikawa and Watanabe [20, Eq. (20)], Kako [21, Eq. (62)] and Taniuti [22, Eqs. (6.9)]. There, the summation over l in Eq. (5) extends harmlessly up to ∞. Though not essential for the issues being investigated in this work, taking the terms $\varepsilon^m V_1^{(m)} e^{i\theta}$, $m \in \mathbb{N} \setminus \{0, 1\}$ into consideration is required for both the elimination of secular terms at higher perturbation orders and the consistent truncation of the general expansion Eq. (5) from which those *Ansätze* derive.

Due to the introduction of the fast and slow variables, the time-derivative operator is transformed according to [23]

$$\frac{d}{dt} = -\omega \frac{\partial}{\partial \theta} - \varepsilon\mu \frac{\partial}{\partial \xi} + \varepsilon^2 \frac{\partial}{\partial \tau}. \tag{6}$$

Upon substituting Eq. (4) into Eq. (2), and then using Eq. (6), we obtain an equation which can be put in the form of a complex Fourier series in the variable θ as follows:

$$F_0(\xi, \tau; k, \varepsilon) + \sum_{l \geqslant 1} F_l(\xi, \tau; k, \varepsilon) e^{li\theta} + \text{c.c.} = 0. \tag{7}$$

The fulfillment of this equation obviously requires that $F_0 = F_l = 0$. The latter actually form a system of coupled nonlinear differential difference equations in ξ and τ whose analytical solutions are not easy to obtain. But thanks to the assumed smallness of ε, we reduce them to only PDEs by performing power series expansion of the form

$$Z(\xi + \eta\varepsilon, \tau) = Z(\xi, \tau) + \sum_{l=1}^{\infty} \frac{(\eta\varepsilon)^l}{l!} \frac{\partial^l Z(\xi, \tau)}{\partial \xi^l} \tag{8}$$

for any of the modulation quantities A, B, C, G_{j0}, and E_{jl} that appear in Eq. (4). Then, keeping the linear relations in Eq. (3) in mind and using the above with $\eta = \pm 1$, we find that F_1 is given to order ε^4 by

$$2\varepsilon^2\alpha\omega^2 G_{10}A + \varepsilon^3\left[\widetilde{P}\frac{\partial^2 A}{\partial \xi^2} - 2i\omega\frac{\partial A}{\partial \tau} + 2\alpha\omega^2(E_{22}\overline{A} + G_{20}A) - 4i\alpha\mu\omega\frac{\partial}{\partial \xi}(G_{10}A) + 2\alpha\omega^2 G_{10}B\right]$$
$$+ \varepsilon^4\left[2\alpha\omega^2(E_{32}\overline{A} + E_{22}A\overline{B} + G_{20}B + G_{30}A) + \widetilde{P}\frac{\partial^2 B}{\partial \xi^2} - 2i\omega\frac{\partial B}{\partial \tau} - 2\mu\frac{\partial^2 A}{\partial \xi \partial \tau} - i\frac{\mu}{6}\frac{\partial^3 A}{\partial \xi^3} - 4i\alpha\omega\mu\frac{\partial}{\partial \xi}(E_{22}\overline{A} + G_{20}A)\right.$$
$$\left. + 4i\alpha\omega\frac{\partial}{\partial \tau}(G_{10}A) - 4i\alpha\mu\omega\frac{\partial}{\partial \xi}(G_{10}B) 2\alpha\omega^2 G_{10}C - 2\alpha\mu^2\frac{\partial^2}{\partial \xi^2}(G_{10}A)\right] = 0, \tag{9}$$

where $\widetilde{P} = \mu^2 - u_0^2 + (\omega^2 + \omega_0^2)/2$. It is worth noticing from this stage that if the bias terms G_{j0} and the coefficients of the higher-order harmonics E_{jl} are taken *a priori* equal to zero for any reason, including in particular the narrowness of the bandpass, then the above equation reduces to one that contains only linear terms involving partial derivatives of A and B. Therefore, the equations that describe the propagation of modulated waves in the electrical line in consideration would be linear dispersive PDEs. We point out that this conclusion still holds even if the *Ansatz* in Eq. (4) is of order ε^0. This case can in effect be deduced from Eq. (34) in Sec. V by taking the limit when both of the coefficients a_2 and a_4 of the higher-order nonlinear terms considered there equal zero. Similarly, each of the various key envelope equations derived elsewhere for a generalized version of our model [14,23] reduces to a linear PDE if the additional model parameters that have not

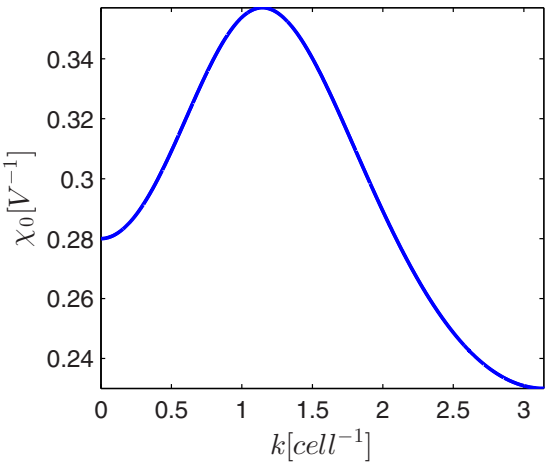

FIG. 3. Variation of the coefficient of the second harmonics with the wave number. Its maximum is attained at $k_\chi \approx 1.15$.

been considered here are equated to zero in the coefficients of that equation. Clearly, such equations lack the nonlinearity which is well known to be indispensable for sustaining the propagation of modulated solitary waves predicted below by our analysis and further confirmed in Sec. IV by our numerical investigations.

With the expansion defined by Eq. (8), each of the Fourier coefficients F_l in Eq. (7) is a power series similar to Eq. (9). We obtain the expression of G_{j0} and E_{jl} as functions of A and B (and eventually their derivatives) by equating the coefficient of ε^j terms of F_l to zero. Thus we have

$$G_{10} = 0, \quad G_{20} = 0, \quad G_{30} = 0, \quad E_{22} = \chi_0 A^2, \tag{10a}$$

$$E_{32} = 2\chi_0 AB + i\chi_1 A\frac{\partial A}{\partial \xi}, \quad E_{33} = \chi_2 A^3. \tag{10b}$$

The quantities $\chi_0 - \chi_2$ are all real constants that depend only on the electrical line parameters ω_0, u_0, and α as well as on the angular frequency ω of the carrier wave. Their expressions are explicitly given as follows:

$$\begin{aligned}
\chi_0 &= \frac{4u_0^2\alpha\omega^2}{\omega^4 - 2\omega_0^2\omega^2 + \omega_0^4 + 3\omega_0^2u_0^2},\\
\chi_1 &= \frac{8u_0^2\alpha\omega\mu\left(\omega^4 - \omega_0^4 - 3\omega_0^2\omega^2\right)}{\left(\omega^4 - 2\omega_0^2\omega^2 + \omega_0^4 + 3\omega_0^2u_0^2\right)^2},\\
\chi_2 &= -\frac{72u_0^6\alpha^2\omega^4}{\left(\omega^4 - 2\omega_0^2\omega^2 + \omega_0^4 + 3\omega_0^2u_0^2\right)\Delta}
\end{aligned} \tag{11a}$$

with

$$\Delta = \left(\omega^2 - \omega_0^2\right)^3 - 6u_0^2\left(\omega^2 - \omega_0^2\right)^2 - 8\omega_0^2u_0^4. \tag{11b}$$

The coefficient χ_0 is of interest for the issue discussed in this paper as it is a factor of the amplitude E_{22} of the second harmonics. Its graphical representation is given in Fig. 3.

We note from Eqs. (10) that, when the reductive perturbation is consistently applied, the bias component of the wave vanishes for the current model (up to the third order of approximation: $G_{10} = G_{20} = G_{30} = 0$) as was pointed out in Ref. [24]. This is, however, not linked to the narrowness of our model, but rather to the specific form of its equation of motion, Eq. (2), where the nonlinear term appears under the time-derivative operator. The situation would be completely different for, e.g., the DNA models investigated in Refs. [13,15] using the RWA.

By substituting Eqs. (10) above into Eq. (9), we find that the dynamics of modulated waves in our model is governed to second order of perturbations by the following system of PDEs:

$$i\frac{\partial A}{\partial \tau} + P\frac{\partial^2 A}{\partial \xi^2} + QA|A|^2 = 0, \tag{12a}$$

$$\begin{aligned}
&i\frac{\partial B}{\partial \tau} + P\frac{\partial^2 B}{\partial \xi^2} + Q(2|A|^2B + A^2\overline{B})\\
&\quad = -R_0\frac{\partial^2 A}{\partial \xi\,\partial \tau} - i\left(\frac{\mu}{6}\frac{\partial^3 A}{\partial \xi^3} + R_1A^2\frac{\partial \overline{A}}{\partial \xi} + R_2|A|^2\frac{\partial A}{\partial \xi}\right),
\end{aligned} \tag{12b}$$

where

$$\begin{aligned}
P &= \frac{\omega_0^2 + 2u_0^2 - \omega^2 - 2\mu^2}{4\omega},\\
Q &= -\frac{4\alpha^2\omega^3u_0^2}{\omega^4 - 2\omega_0^2\omega^2 + \omega_0^4 + 3\omega_0^2u_0^2},\\
R_0 &= \frac{\mu}{\omega},\\
R_1 &= \frac{8\mu\alpha^2\omega^2u_0^2}{\omega^4 - 2\omega_0^2\omega^2 + \omega_0^4 + 3\omega_0^2u_0^2},\\
R_2 &= \frac{8\mu\alpha^2\omega^2u_0^2\left(3\omega_0^4 + \omega^4 + 9\omega_0^2u_0^2 - 4\omega_0^2\omega^2\right)}{\left(\omega^4 - 2\omega_0^2\omega^2 + \omega_0^4 + 3\omega_0^2u_0^2\right)^2}.
\end{aligned} \tag{13}$$

In particular, Eq. (12a) is the standard nonlinear Schrödinger (NLS) equation which is well known to be derivable at first order of perturbations from similar models, using an *Ansatz* that includes just the terms $\varepsilon Ae^{i\theta} + \varepsilon^2E_{22}e^{2i\theta}$ + c.c. in our notation [17]. Consistently with this fact, these two terms turn out here to be the only ones of our more general *Ansatz* (4) that effectively contribute to the standard NLS. In effect, we obtain Eq. (12a) by setting the ε^3 term of Eq. (9) to zero. The latter appears to depend on G_{10}, G_{20}, and B in addition to E_{22}. But considering Eqs. (10), only E_{22} which is nonzero and not proportional to the null terms G_{10} and G_{20} will be left. In fact, letting the cubic coefficient β not considered here equal to zero in Ref. [17, Eqs. (2.10)] and further eliminating the wave number by appropriately exploiting Eqs. (2.3) and (2.5) of the same paper reduce the expressions of P and Q therein to those in Eq. (13) above.

Up to now, B remains arbitrary. It could then be taken equal to zero as in existing works if our final solution were to retain only the ε term of the assumed *Ansatz*. However, as one of the aims of this work is to check whether higher-order harmonic components of a given wave would propagate in our narrow spectrum network, it is necessary to explicitly include at least one such harmonic in the solution retained. For simplicity, one can consider the second harmonic $E_{22}e^{2i\theta}$ which happens to be already known. Now, all the terms of the *Ansatz* that appear at the same order of perturbation as $E_{22}e^{2i\theta}$ must equally be determined for mathematical *consistency*.

This implies in our case that an equation that fixes B is needed. Conforming rigorously with the spirit of perturbation theory according to which each perturbation term of a given equation must independently be equated to zero, we obtain the required equation as Eq. (12b) from the ε^4 term of Eq. (9); obviously upon substitution of Eqs. (10).

It is interesting to observe that the process of equating each ε term of Eq. (9) to zero would lead to a system of two different nonlinear PDEs for the same quantity A if one omits the B term in the *Ansatz* (4). In this case, the solution of any of these PDEs *must also* verify the other PDEs in order to be an acceptable approximate solution for the original discrete equation (2). This is certainly a strong constraint that can preclude the existence of solutions. For the low-pass counterpart of our nonlinear transmission line (NLTL), which is obtained by removing the parallel inductor L_p from the circuit (leading to $\omega_0 = 0$ in the corresponding model equation), Ref. [18] presents a second-order analysis where the B term is omitted. There, the constraint just mentioned is bypassed by considering Eq. (9) as a whole, single equation that formally consists of the left-hand side of Eq. (12a) equated to ε times the right-hand side of Eq. (12b). Some similarities can thus be expected between the coefficients in this paper and those obtained therein. This is effectively the case: By letting $\omega_0 = 0$ in Eq. (13), the expressions of our P and Q become those in Ref. [18, Eqs. (2.7)] while those of R_0, R_1, and R_2 reduce to the respective coefficients in the right-hand side of Eq. (2.6) of the same paper. Under $\omega_0 = 0$, the expression of χ_0 in Eq. (11) of this paper is also reduced to the coefficient in the definition of B in [18, Eqs. (2.8)]. One of the advantages of the coupled form given by Eqs. (12) is that it enables one to obtain some exact and fully explicit analytical solutions as will be seen in the next section. This is contrary to [18, Eq. (2.6)] where the effects of the higher-order analysis could be appreciated only through some averaging procedure. The latter is approximate and can easily be applied to bright solitons only.

Just like the necessity of including the terms $\varepsilon^m V_1^{(m)} e^{i\theta}$, $m \in \mathbb{N} \setminus \{0, 1\}$ in the *Ansätze* is recognized at least since the 1970s [20–22], the approach whose developments have led us to Eqs. (12) is nothing new. It was used by Ichikawa *et al.* to investigate the contribution of higher-order terms in the reductive perturbation theory for strongly dispersive waves [25]. For the physical problem that they examined and which consisted of an ion-plasma wave, they obtained their Eq. (33.a) and Eq. (33.b) as the respective counterparts to our Eqs. (12a) and (12b). In a relatively recent work by Demiray, one can observe that the lowest-order term in the expansion is governed by the nonlinear Schrödinger equation while the second-order term is governed by the linear Schrödinger equation [26, Eqs. (15) and (19)]. This is once again in accordance with our Eqs. (12a) and (12b), respectively.

III. EXACT ANALYTICAL SOLUTIONS

This section is devoted to the investigation of some solutions of the system of coupled PDEs derived from the discrete equation of our NLTL. In general, the dependent functions A and B can be expressed in polar form according to

$$\begin{aligned} A(\xi, \tau) &= a(\xi, \tau) e^{i\phi(\xi,\tau)}, \\ B(\xi, \tau) &= b(\xi, \tau) e^{i[\phi(\xi,\tau)+\psi(\xi,\tau)]}, \end{aligned} \tag{14}$$

where a and ϕ are real-valued functions representing the amplitude and phase of A while b is the amplitude of B and ψ a possible phase difference relative to A. Introducing these relations into Eqs. (12) and separating each of the latter into real and imaginary parts lead to the system of PDEs given below:

$$P\frac{\partial^2 a}{\partial \xi^2} - a\frac{\partial \phi}{\partial \tau} - Pa\left(\frac{\partial \phi}{\partial \xi}\right)^2 + Qa^3 = 0, \tag{15a}$$

$$\frac{\partial a}{\partial \tau} + 2P\frac{\partial \phi}{\partial \xi}\frac{\partial a}{\partial \xi} + Pa\frac{\partial^2 \phi}{\partial \xi^2} = 0, \tag{15b}$$

$$\begin{aligned} &\frac{\mu}{6}a\left[\left(\frac{\partial \phi}{\partial \xi}\right)^3 - \frac{\partial^3 \phi}{\partial \xi^3}\right] - \frac{\mu}{2}\frac{\partial}{\partial \xi}\left(\frac{\partial \phi}{\partial \xi}\frac{\partial a}{\partial \xi}\right) + R_0\left(\frac{\partial^2 a}{\partial \xi \partial \tau} - a\frac{\partial \phi}{\partial \xi}\frac{\partial \phi}{\partial \tau}\right) + (R_1 - R_2)a^3\frac{\partial \phi}{\partial \xi} \\ &\quad - \left[Pb\left(\frac{\partial^2 \phi}{\partial \xi^2} + \frac{\partial^2 \psi}{\partial \xi^2}\right) + \frac{\partial b}{\partial \tau} + 2P\left(\frac{\partial \phi}{\partial \xi} + \frac{\partial \psi}{\partial \xi}\right)\frac{\partial b}{\partial \xi}\right]\sin(\psi) \\ &\quad + \left[3Qa^2 b - P\left(\frac{\partial \phi}{\partial \xi}\right)^2 - P\left(\frac{\partial \psi}{\partial \xi}\right)^2 - b\left(\frac{\partial \phi}{\partial \tau} + \frac{\partial \psi}{\partial \tau}\right) - 2Pb\frac{\partial \phi}{\partial \xi}\frac{\partial \psi}{\partial \xi} + P\frac{\partial^2 b}{\partial \xi^2}\right]\cos(\psi) = 0, \end{aligned} \tag{15c}$$

$$\begin{aligned} &(R_1 + R_2)a\frac{\partial a}{\partial \xi} + \frac{\mu}{6}\frac{\partial^3 a}{\partial \xi^3} + R_0\left(\frac{\partial \phi}{\partial \tau}\frac{\partial a}{\partial \xi} + \frac{\partial \phi}{\partial \xi}\frac{\partial a}{\partial \tau} + a\frac{\partial^2 \phi}{\partial \xi \partial \tau}\right) - \frac{\mu}{2}\left[\left(\frac{\partial \phi}{\partial \xi}\right)^2\frac{\partial a}{\partial \xi} + a\frac{\partial \phi}{\partial \xi}\frac{\partial^2 \phi}{\partial \xi^2}\right] \\ &\quad + \left[P\frac{\partial^2 b}{\partial \xi^2} - b\left(\frac{\partial \phi}{\partial \tau} + \frac{\partial \psi}{\partial \tau}\right) - Pb\left(\frac{\partial \psi}{\partial \xi}\right)^2 - Pb\left(\frac{\partial \phi}{\partial \xi}\right)^2 + Qa^2 b - 2Pb\frac{\partial \psi}{\partial \xi}\frac{\partial \phi}{\partial \xi}\right]\sin(\psi) \\ &\quad + \left[Pb\left(\frac{\partial^2 \psi}{\partial \xi^2} + \frac{\partial^2 \phi}{\partial \xi^2}\right) + \frac{\partial b}{\partial \tau} + 2P\left(\frac{\partial \phi}{\partial \xi} + \frac{\partial \psi}{\partial \xi}\right)\frac{\partial b}{\partial \xi}\right]\cos(\psi) = 0. \end{aligned} \tag{15d}$$

A. Modulational instability

The simplest solutions worth of consideration for the analysis of wave propagation in our NLTL correspond to the so-called plane waves. Their characteristics are the constancy of their amplitudes and the linear dependency of their phases on space and time. Seeking such solutions for Eqs. (15), we take $a(\xi,\tau)=A_0$, $b(\xi,\tau)=B_0$, $\phi(\xi,\tau)=\kappa\xi-\Omega\tau$ and assume a constant phase difference $\psi(\xi,\tau)=\psi_0$. Then we find that the amplitudes A_0 and B_0 of the plane waves and their angular pulsation Ω and wave number κ verify

$$\Omega = P\kappa^2 - QA_0^2,$$
$$B_0 = \frac{\left[6(R_0Q - R_1 + R_2)A_0^2 - (6R_0P+\mu)\kappa^2\right]\kappa}{12QA_0\cos(\psi_0)}. \quad (16)$$

We see that the B_0 can exist only for $\psi_0 \neq \pm\pi/2$ and is moreover relevant for $\kappa \neq 0$.

To study the linear stability of these plane waves, we consider small perturbations to their amplitudes and phases according to

$$a(\xi,\tau) = A_0 + \epsilon a_1(x,t), \quad \phi(\xi,\tau) = \kappa\xi - \Omega\tau + \epsilon\phi_1(x,t),$$
$$b(\xi,\tau) = B_0 + \epsilon b_1(x,t), \quad \phi(\xi,\tau) = \psi_0 + \epsilon\psi_1(x,t). \quad (17)$$

We introduce these expressions into Eqs. (15) which we subsequently expand in power series of ϵ. Taking Eqs. (16) into account, the order ϵ^0 of each of these series vanishes. Equating the coefficients of the leading terms of what remain to zero forms a system of linear PDEs that govern the dynamics of the perturbations. The solutions of the latter system of PDEs are sought in the form

$$\begin{pmatrix} a_1(\xi,\tau)\\ \phi_1(\xi,\tau)\\ b_1(\xi,\tau)\\ \psi_1(\xi,\tau)\end{pmatrix} = \begin{pmatrix} a_{10}\\ \phi_{10}\\ b_{10}\\ \psi_{10}\end{pmatrix} e^{i(\lambda\xi-\nu\tau)}, \quad (18)$$

where a_{10}, ϕ_{10}, b_{10}, and ψ_{10} are constants. This leads to a homogeneous system of linear algebraic equations

$$\begin{pmatrix} \Gamma_1 & \Gamma_2 & 0 & 0\\ \Gamma_3 & \Gamma_4 & 0 & 0\\ \Gamma_5 & \Gamma_6 & \Gamma_7 & \Gamma_8\\ \Gamma_9 & \Gamma_{10} & \Gamma_{11} & \Gamma_{12}\end{pmatrix}\begin{pmatrix} a_{10}\\ \phi_{10}\\ b_{10}\\ \psi_{10}\end{pmatrix} = \begin{pmatrix} 0\\ 0\\ 0\\ 0\end{pmatrix}. \quad (19)$$

The Γ's are complex-valued expressions that are extremely cumbersome and are not given to save space. Using these expressions and taking Eqs. (16) into account, the solvability condition of Eq. (19), namely, that the determinant of its matrix vanishes identically, is found to be

$$\left[\nu^2 - 4P\lambda\kappa\nu + P\lambda^2\left(2QA_0^2 - P\lambda^2 + 4P\kappa^2\right)\right]^2 = 0. \quad (20)$$

Equation (20) is equivalent to $\nu^2 - 4P\lambda\kappa\nu + P\lambda^2(2QA_0^2 - P\lambda^2 + 4P\kappa^2) = 0$ and is merely the same equation yielded by MI investigation for the standard NLS equation alone.

We can then deduce that plane-wave solutions with properties given by Eqs. (16) can become modulationnally unstable in our model only if the product of the two coefficients P and Q of Eq. (12a) is positive. The graphs of the latter are given in Fig. 4. It is observed that the coefficient P of linear dispersion decreases monotonically from positive to negative values as a function of the wave number, vanishing at a critical value

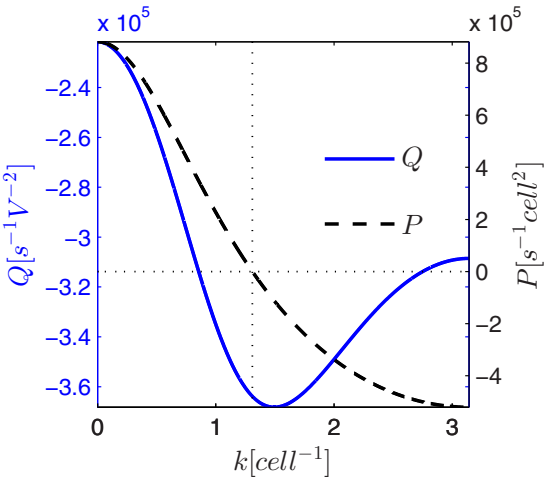

FIG. 4. Variation of the coefficients of linear dispersion P and of cubic nonlinearity Q as functions of wave number. The product PQ is seen to be negative for $k < k_c$ and positive for $k_c < k$ with $k_c \approx 1.31$.

$k_c \approx 1.31$ of the wave number (the corresponding frequency is $f_c \approx 0.781$ MHz). As for the coefficient Q of the cubic nonlinearity, it remains negative within the first Brillouin zone. The MI of plane waves can thus develop for wave numbers in the range $k_c < k \leqslant \pi$.

B. Solitary wave solutions

The class of solutions we are mostly interested in is that of localized nonlinear waves. We restrict ourselves to the cases where the real amplitudes $a(\xi,\tau)$ and $b(\xi,\tau)$ are independent of τ while $\phi(\xi,\tau)=\sigma\tau$ and $\psi(\xi,\tau)=\pi/2$. Then, defining a function $\tilde{f}$ in terms of a as

$$\tilde{f} = \frac{\mu}{6}a''' + [(R_1+R_2)a^2 + R_0\sigma]a', \quad (21a)$$

the system of couples PDEs in Eqs. (15) reduces to the following system of coupled ordinary differential equations:

$$Pa'' - \sigma a + Qa^3 = 0, \quad (21b)$$
$$Pb'' + (Qa^2 - \sigma)b + \tilde{f} = 0. \quad (21c)$$

Above, a prime ($'$) denotes a differentiation with respect to ξ. Equation (21b) is the famous cubic Duffing oscillator equation and is one of the most studied equations of physical sciences. Depending on the signs of its coefficients, it can admit periodic or bounded hyperbolic solutions. The expressions of each of these types of solution can be obtained analytically in terms of the Jacobian elliptic functions or hyperbolic functions, respectively. On the other hand, it is easy to verify that a solution, a, of Eq. (21b) is also a solution of the homogeneous equation associated with Eq. (21c). Thus, by classical routine [27,28], one obtains the complete solution of the latter formally as

$$b(\xi) = \left[\rho_1 + \int^{\xi}\tilde{a}(s)\tilde{f}(s)ds\right]a(\xi) + \left[\rho_2 - \int^{\xi}a(s)\tilde{f}(s)ds\right]\tilde{a}(\xi), \quad (22a)$$

where ρ_1 and ρ_2 are arbitrary constants and

$$\tilde{a}(\xi) = a(\xi) \int \frac{d\xi}{a^2(\xi)}. \tag{22b}$$

This last function is not bounded in general; so the constants ρ_1 and ρ_2 have to be chosen appropriately in order to keep the variation of b finite. The final approximate expression for the voltage in our NLTL, valid to order $O(\varepsilon^3)$ is formally given by

$$\begin{aligned} V_n(t) = {} & 2\varepsilon a(\xi)\cos[kn - (\omega - \varepsilon^2\sigma)t] \\ & - 2\varepsilon^2 b(\xi)\sin[kn - (\omega - \varepsilon^2\sigma)t] \\ & + 2\chi_0\varepsilon^2 a^2(\xi)\cos\{2[kn - (\omega - \varepsilon^2\sigma)t]\} \end{aligned} \tag{23}$$

with $\xi = \varepsilon(n - \mu t)$. In particular, for $PQ > 0$, we have

$$a(\xi) = a_0 \operatorname{sech}\left(\xi a_0 \sqrt{\frac{Q}{2P}}\right), \quad \sigma = \frac{a_0^2 Q}{2}, \tag{24a}$$

$$b(\xi) = \left[\delta_0 - \delta_1 a_0 \xi + \delta_2 \tanh\left(\xi a_0 \sqrt{\frac{Q}{2P}}\right)\right] a_0 a(\xi), \tag{24b}$$

which corresponds to the bright type soliton. Here, a_0 is an arbitrary constant that determines the amplitude of the pulse while δ_0, δ_1, and δ_2 depend on the parameters of Eqs. (12) as follows:

$$\begin{aligned} \delta_0 &= \frac{12(R_1 + R_2)P - 7\mu Q - 6PQR_0}{48P^2}\sqrt{\frac{2}{PQ}}, \\ \delta_1 &= \frac{(\mu + 6PR_0)}{24P^3}, \\ \delta_2 &= \frac{\mu Q - 2(R_1 + R_2)P}{8P}\sqrt{\frac{2}{PQ}}. \end{aligned} \tag{25}$$

We notice here that, if Eqs. (24) are substituted into Eq. (23), the arbitrary parameter ε can be consistently absorbed into the amplitude a_0 of the pulse.

IV. NUMERICAL ANALYSIS

In this section, we conduct a numerical investigation of the propagation status of the approximate solutions derived in the preceding section. Our fundamental concern here is to check whether the modulated wave given in Eq. (23), which has been possible to predict analytically only by considering higher-order harmonics as already pointed out herein, do effectively propagate in our narrow bandpass NLTL. And in the case it does, we also aim to know whether the second-order harmonic retained is transmitted through this network.

The wave's frequency obviously turns out to be the key quantity to consider for this investigation. So the results presented below are obtained with the fixed value $a_0 = 0.1$ V of the wave's amplitude parameter. They are nevertheless typical and not qualitatively affected by changes of a_0 that reasonably maintain the smallness of amplitude assumed in the analytical study (values up to $a_0 = 0.3$ have been checked).

To proceed, we consider a network of $N = 1200$ effective elementary cells. The discrete set of coupled equations governing the voltages in the cells as provided by Eq. (2) are integrated numerically using an explicit Runge-Kutta (4),(5) formula. Specifically, the Dormand-Prince pair [29] as implemented in Matlab's function ode45 is used with a stringent relative tolerance of about 5×10^{-10}. We choose the initial conditions as

$$V_n(t_0) = \dot{V}_n(t_0) = 0, \quad n = 1, \ldots, N \tag{26}$$

and excite the left end of the lattice with a signal $V_0(t)$. We employ two strategies in order to reduce as much as possible the effects of the reflection of waves at the other end of the lattice.

First, the forward time integration is performed only for a duration just equal to the theoretical value $T_{\max} = 0.75N/\mu$ required for an input wave to propagate through 75% of the lattice. Assuming a possible mismatch between the theoretical and the actual propagation speeds, we further implement the so-called absorbing boundary condition [30]. Thus, the effective network is extended with some 120 extra cells whose dynamical equations additionally include a viscous damping term $\gamma(n)\dot{V}_n$. The damping coefficient $\gamma(n)$ increases with position according to

$$\gamma(n) = 5\left[1 + \tanh\left(\frac{n - N - 60}{4}\right)\right], \quad N < n \leqslant N + 120 \tag{27}$$

so that any incoming wave is progressively damped out beyond the last cell considered to be part of the effective network.

We begin with a look at the behavior of a plane wave whose parameters fulfill the theoretical condition required for its modulational instability. For this purpose, the input signal is taken following [18] in the form

$$V_0(t) = 2a_0[1 + r\cos(\nu t)]\cos(\varpi t). \tag{28}$$

Tracing from the definitions of the phase of the carrier wave ($\theta = kn - \omega t$), the phase of the envelope wave [$\phi(\xi, \tau) = \kappa\xi - \Omega\tau$] and Eqs. (16), we calculate here the angular frequency ϖ for a wave number $k > k_c$ according to $\varpi = \omega + \kappa^2 P - Qa_0^2$ with ω obeying the dispersion relation in Eq. (3) and P and Q given by Eqs. (13). The modulating signal of amplitude r and angular frequency ν figures a small perturbation for $0 < r \ll 1$. Theoretically, the quasi plane wave respesented by Eq. (28) will develop an instability during its propagation if the value of ν is such that Eq. (20) admits complex solutions for λ. We present in Fig. 5 an illustration of the confirmation of the predicted phenomenon. This figure is obtained by numerically integrating Eq. (2) with the input signal (28) and the initial conditions (26) with $t_0 = 0$.

Turning now to the actual investigation of the propagation of the modulated solution (23) and (24), the input signal $V_0(t)$ is deduced from the expression of this solution by setting $n = 0$. Then, the initial time t_0 is (theoretically) taken to be $-\infty$ in order that the whole shape of the pulse forms from the function $V_0(t)$.

For a given value of the frequency f_p, the first and elementary means we adopt for ascertaining the propagation consists of recording the position of the wave front at different time instants. An example of such a stroboscopic view is provided in Fig. 6 for our electrical lattice. This plot, which corresponds to $f_p = 1.015$ MHz, or equivalently $k_p = 3$, reveals undoubtedly that the input pulse moves down the network as time evolves.

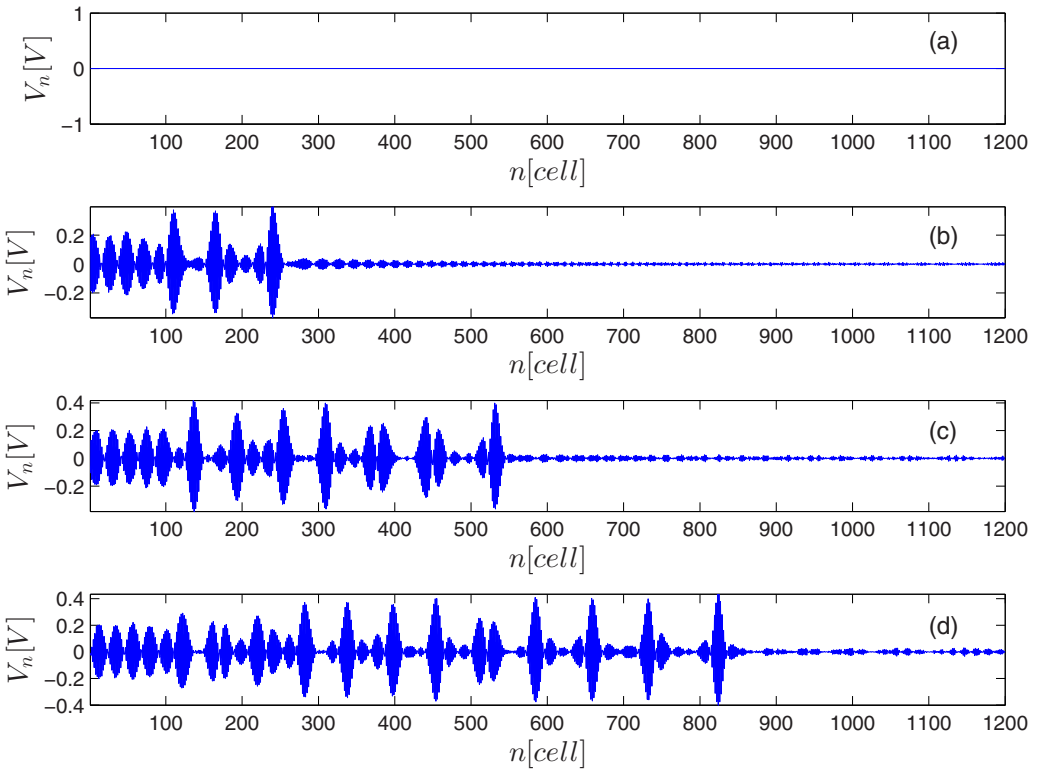

FIG. 5. Development of MI in the network for the frequency value $f_p = 1.015$ MHz and for $\kappa = 0$, $a_0 = 0.1$, $r = 0.001$, and $\nu = \pi f_p/50$. The subplots display the state of the network at (a) $t = 0$, (b) $t = 0.25N/\mu$, (c) $t = 0.50N/\mu$, and (d) $t = 0.75N/\mu$.

We next consider the famous spectral analysis for a quantitative analysis of the propagation. Here we monitor the amplitude $|\widetilde{S}(f)|$ of the Fourier transform (FT)

$$\widetilde{S}(f) = \frac{1}{\sqrt{2\pi}} \int_{-\infty}^{\infty} S(t) e^{-i2\pi ft} dt \tag{29}$$

of the wave signal $S(t)$. Concretely, we sample the time dependence of the voltages in 50 distinct cells that are regularly spaced along the effective network during the numerical integration. The sampling time Δt is calculated in a way to collect a total of 32 768 data (for each of those 50 cells) evenly distributed over the whole integration time defined above. Finally, we use the standard fast Fourier transform algorithm to numerically compute the FT for the data collected. Figure 7 illustrates the outcome of this procedure for the particular cell $n = 504$. At first glance, the FT profile looks very similar to that of a harmonic signal because its seems to contain a single peak [see Fig. 7(b)]. The apparent absence of higher harmonic components is well understandable from the analytical considerations. In effect the second harmonic component, which is expected to have the highest amplitude of them, scales as the product $\chi_0 a_0^2$ with $a_0 \ll 1$ and, for the current value of the frequency, $\chi_0 < 0.25$ [see Eqs. (10a) and (23), and Fig. 3]. Actually, a closer look at the spectrum around the fundamental and the second-order frequencies of the input signal reveals the pulse-shaped form of the FT profile around each of these frequencies, as can be seen from Figs. 7(c) and 7(d). One can

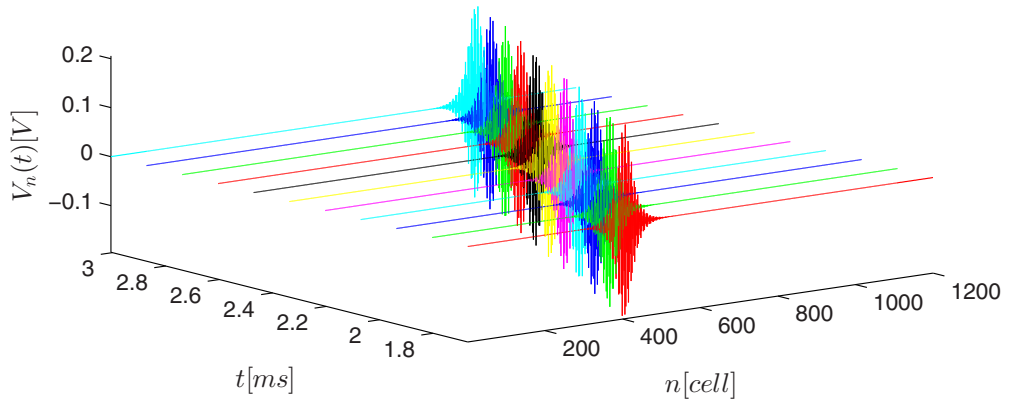

FIG. 6. A three-dimensional representation of the stroboscopic view of the network status for the frequency value $f_p = 1.015$ MHz.

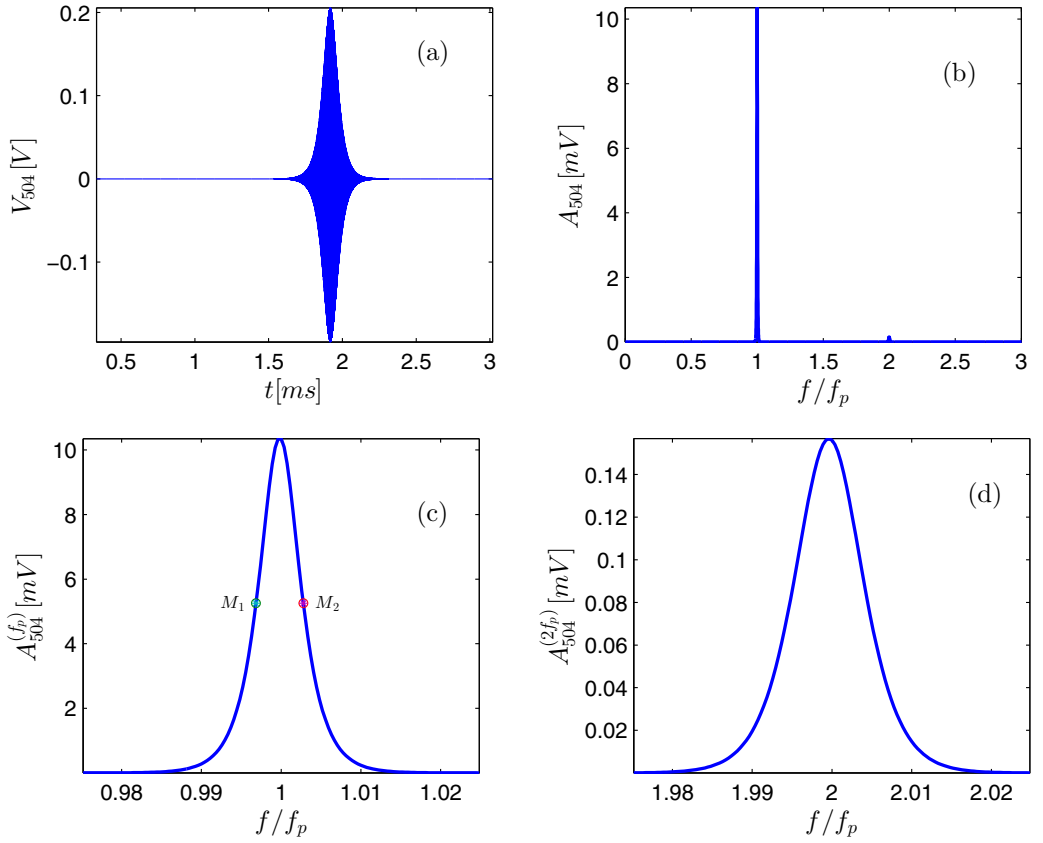

FIG. 7. Illustration of (a) the voltage waveform and (b) its Fourier transform at cell 504 for the frequency value $f_p = 1.015$ MHz. Parts (c) and (d) are zooms of (b) around $f = f_p$ and $f = 2f_p$, respectively. The distance between the symmetric points M_1 and M_2 located at half maximum of the pulse constitutes the full width at half maximum.

characterize the quality of the propagation by studying the variations of the amplitudes and full widths at half maximum (FWHM) of these two pulses during the propagation of the signal. Thus, we repeat the calculations just described for all of the 50 cells of our sample and extract the characteristics of interest to obtain the plots of Fig. 8. Figure 8(a) shows that the amplitudes of the pulses at both the fundamental and second frequencies are nonzero and constant for cells up to approximately $n \approx 850$, which are certainly those traversed by the pulse. Beyond this interval, they decrease simultaneously and become zero in the same ranges. Figure 8(b) proves that the first and second frequency FWHMs are equal and, more importantly, also constant for cells traversed by the electrical pulse signal. These two graphs conspicuously

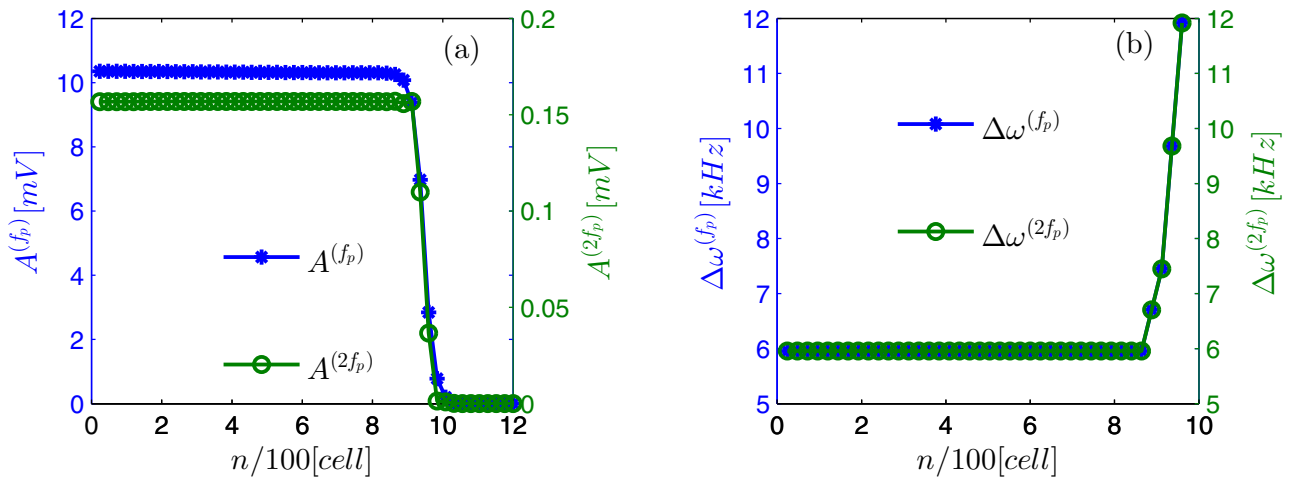

FIG. 8. Variation along the network of (a) the amplitude and (b) the full width at half maximum of the pulses at the first and second harmonics.

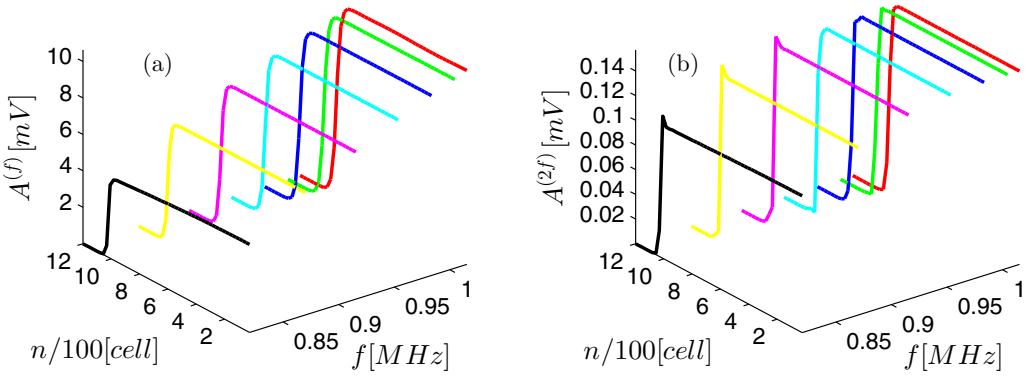

FIG. 9. Effect of frequency on the variation of the pulse amplitude at the (a) first and (b) second harmonics.

demonstrate that the second harmonic component of the wave is transmitted with preservation of its shape and amplitude, just like the first harmonic component.

The frequency value $f_p = 1.015$ MHz considered up to now is actually quite close to the cutoff frequency. So its first multiple will be farther out of band. This makes it a very good candidate for drawing some observations on the issue which is the subject of this work. To turn these observations into reliable conclusions we have repeated the analysis detailed above for other frequencies. The main results are portrayed in Figs. 9(a) and 9(b) confirming that the observations made previously are not simple artifacts that are peculiar to the frequency value $f_p = 1.015$ MHz.

V. FURTHER DISCUSSION

Up to this point, our analysis has focused on the NLTL of Fig. 1 when it is assumed to be governed by Eq. (2). In spite of the fact that its linear spectrum is narrow, which makes it suitable for investigation by the RWA according to currently accepted claims, we have noted in Sec. II that this technique is inappropriate for this purpose due to its stringent failure to predict nonlinear modulated waves that are yet supported by the model as demonstrated above. The following observation further sheds light on the fact that the narrowness of the linear spectrum band is not the prevailing reason that should prompt the use of the RWA.

The capacitance voltage relationship of our model is often taken as [31]

$$C_b(V_n) = C_0\left[1 + \sum_{s=1}^{5}(-1)^s(s+1)a_s V_n^s\right] \tag{30}$$

with

$$a_1 = 0.2\ \mathrm{V}^{-1}, \quad a_2 = 0.0257\ \mathrm{V}^{-2}, \quad a_3 = 0.002\,22\ \mathrm{V}^{-3},$$
$$a_4 = 1.22\times10^{-4}\ \mathrm{V}^{-4}, \quad a_5 = 3.5\times10^{-6}\ \mathrm{V}^{-5} \tag{31}$$

still for the dc bias voltage $V_b = 2$ V. Equation (30) with the values in Eq. (31) is considered to fit more accurately the exact characteristic of the BB112 reversed-biased diode than Eq. (1). For this higher-order polynomial approximation, the discrete equations of motion of the NLTL of Fig. 1 become

$$\frac{d^2}{dt^2}\left(V_n + \sum_{s=1}^{5}(-1)^s a_s V_n^{s+1}\right) + u_0^2(2V_n - V_{n+1} - V_{n-1}) + \omega_0^2 V_n = 0. \tag{32}$$

Within the RWA which uses the *Ansatz*

$$V(\theta,\xi,\tau) = A(\xi,\tau)e^{i\theta} + \overline{A}(\xi,\tau)e^{-i\theta}, \tag{33}$$

one obtains the extended NLS equation

$$i\frac{\partial}{\partial\tau}(A + 3a_2A|A|^2 + 10a_4A|A|^4) - \frac{\mu^2}{2\omega}\frac{\partial^2}{\partial\xi^2}(A + 3a_2A|A|^2 + 10a_4A|A|^4) - i\frac{\mu}{\varepsilon}\frac{\partial}{\partial\xi}(3a_2A|A|^2 + 10a_4A|A|^4) + \frac{\omega}{2\varepsilon^2}(3a_2A|A|^2 + 10a_4A|A|^4) = 0, \tag{34}$$

as the one governing nonlinear modulated waves in the system. Noticing that the two levels of modeling the network in Fig. 1 have the same linear spectrum but differ only in the degree of nonlinearity considered, the immediate conclusion we can make, and which is valid beyond our NLTL, is that the adequacy of the RWA is attached to the nonlinearity rather than to the width of the linear spectrum. In fact, a careful inspection of the coefficients of Eq. (34) indicates moreover that they involve the coefficients a_2 and a_4 of the odd order terms of Eq. (32), but none of a_1, a_3, and a_5 of its even order terms. This is also true for the envelope equations derived in Refs. [14,23] for a generalized version of our model using the RWA. So, on the one hand, the RWA technique does not account for even order nonlinearities but only for odd order nonlinearities. On the other hand, a basic mathematical analysis on the magnitudes of the nonlinear terms of Eq. (32) with the values in Eq. (31) reveals that its quadratic term is at least 3.89 times stronger than its cubic term. This smallest factor is attained at the dc bias voltage, $V_n = V_b = 2$ V, which is seldom considered to be approached in investigations of our NLTL model. It increases above 15.56 when the voltage decreases below 0.5 V, which is the voltage range commonly considered in those analyse. The reliability of the RWA

technique then appears to be undoubtedly a matter of concern here since weaker effects are accounted for while stronger ones are not. Once again, this observation is not peculiar to the NLTL under consideration. We remark in effect that the polynomial equations of motion to which the RWA is applied in investigations of discrete lattices are usually obtained from polynomial expansions or interpolations of more general and nonpolynomial equations. See [13,15] for some examples. For physically relevant models, the corresponding coefficients decrease with the increase of the order of the nonlinearity, so that lower-order nonlinear terms are stronger than higher-order ones as above. We suggest therefore that, instead of the narrowness of width of the linear spectrum, the presence of only odd order nonlinearities in the model equation should be the principal criterion to consider for using the RWA for an accurate investigation of that model.

VI. CONCLUSION

This paper has discussed the theoretical investigation of modulated waves in one-dimensional nonlinear discrete systems that have a narrow linear bandpass spectrum. An electrical transmission line whose lone nonlinear element is a capacitor with a simple quadratic charge-voltage relationship has been used as a case study. Our analytical analysis has then highlighted the fact that, disregarding higher-order harmonic components in the waves to be propagated in the network leads to barely linear dispersive equations for their envelopes. Solitons bearing equations are obtained on the contrary when the higher-order harmonics are taken into account. For appropriately chosen *Ansatz*, and within the reductive perturbation framework, these equations consist of the standard NLS equation coupled to inhomogeneous linear PDEs. The analytical expressions of their soliton solutions have been obtained explicitly to second order of perturbation. They have been used as input for the numerical integration of the discrete equations of the electrical line and have proved to propagate without distortion. The spectral analysis of the output of the numerical integration data has revealed that the fundamental as well as the second harmonic included in the expression of the solution do propagate throughout the network. For our example of discrete lattice, the magnitude of the latter was found to be so small that careful attention is required to notice its presence from the spectral analysis. Our analytical study, which shows that this magnitude is nonzero in the whole bandwidth, indicates that it depends on both the linear and nonlinear elements of the lattice, respectively, through the angular frequency and the nonlinearity coefficient. For some systems therefore, analyses that rely *a priori* on the narrowness of the linear bandwidth solely to neglect higher-order harmonics and dc bias components will lead at best to inaccurate and, hence, potentially unreliable results and conclusions. This is especially true for models governed by asymmetric equations of motion. On the contrary the RWA seems to be safe from those shortcomings for models governed by symmetric equations of motion.

[1] S. Yomosa, Phys. Rev. A **32**, 1752 (1985).
[2] P. Perez and N. Theodorakopoulos, Phys. Lett. A **117**, 405 (1986).
[3] P. Perez and N. Theodorakopoulos, Phys. Lett. A **124**, 267 (1987).
[4] V. Muto, P. S. Lomdahl, and P. L. Christiansen, Phys. Rev. A **42**, 7452 (1990).
[5] M. Remoissenet, *Waves Called Solitons—Concepts and Experiments*, 3rd ed. (Springer-Verlag, Berlin, 2003).
[6] A. C. Scott, *Nonlinear Science: Emergency and Dynamics of Coherent Structures* (Oxford University Press, Oxford, 1999).
[7] A. M. Gurn, Chaos **13**, 754 (2003).
[8] Y. S. Kivshar, *Optical Solitons: From Fibers to Photonic Crystals* (Academic, San Diego, 2003).
[9] R. Lifshitz and M. C. Cross, Phys. Rev. B **67**, 134302 (2003).
[10] Y. Bromberg, M. C. Cross, and R. Lifshitz, Phys. Rev. E **73**, 016214 (2006).
[11] C. Gardner and G. Morikawa, Commun. Pure Appl. Math. **18**, 35 (1965).
[12] J. M. Bilbault and P. Marquié, Phys. Rev. E **53**, 5403 (1996).
[13] C. B. Tabi, A. Mohamadou, and T. C. Kofané, Phys. Scr. **77**, 045002 (2008).
[14] D. Yemélé and F. Kenmogné, Phys. Lett. A **373**, 3801 (2009).
[15] P. B. Ndjoko, J. M. Bilbault, S. Binczak, and T. C. Kofane, Phys. Rev. E **85**, 011916 (2012).
[16] A. B. Togueu Motcheyo, C. Tchawoua, and J. D. Tchinang Tchameu, Phys. Rev. E **88**, 040901(R) (2013).
[17] P. Marquie, J. M. Bilbault, and M. Remoissenet, Phys. Rev. E **49**, 828 (1994).
[18] D. Yemélé, P. Marquié, and J. M. Bilbault, Phys. Rev. E **68**, 016605 (2003).
[19] F. B. Pelap and M. M. Faye, J. Math. Phys. **46**, 033502 (2005).
[20] Y. Ichikawa and S. Watanabe, J. Phys., Colloq. **38**, C6-15 (1977).
[21] M. Kako, Prog. Theor. Phys. Suppl. **55**, 120 (1974).
[22] T. Taniuti, Prog. Theor. Phys. Suppl. **55**, 1 (1974).
[23] S. B. Yamgoué and F. B. Pelap, Phys. Lett. A **380**, 2017 (2016).
[24] F. Kenmogne, D. Yemélé, and P. Marquié, Phys. Rev. E **94**, 036201 (2016).
[25] Y. H. Ichikawa, T. Mitsuhashi, and K. Konno, J. Phys. Soc. Jpn. **43**, 675 (1977).
[26] H. Demiray, Commun. Nonlinear Sci. Numer. Simul. **10**, 549 (2005).
[27] S. B. Yamgoué and T. C. Kofané, Chaos, Solitons Fractals **15**, 119 (2003).
[28] G. J. Gbur, *Mathematical Methods for Optical Physics and Engineering* (Cambridge University Press, Cambridge, UK, 2011).
[29] J. R. Dormand and P. J. Prince, J. Comput. Appl. Math. **6**, 19 (1980).
[30] S. B. Yamgoué, S. Morfu, and P. Marquié, Phys. Rev. E **75**, 036211 (2007).
[31] K. Tse Ve Koon, J. Leon, P. Marquié, and P. Tchofo-Dinda, Phys. Rev. E **75**, 066604 (2007).